Enhancing the Gas-Sensing Properties of $(RuPc)_2$ Thin Films by Thermally Induced Morphological Stabilizing Effects

Amanda Generosi, Barbara Paci, Valerio Rossi Albertini, Renato Generosi, Paolo Perfetti, Anna Maria Paoletti, Gianna Pennesi, Gentilina Rossi, and Ruggero Caminiti

Istituto di Struttura della Materia, CNR, Via del Fosso del Cavaliere 100, 00133 Roma, Italy, Istituto di Struttura della Materia, CNR, Via Salaria Km.29.5, Monterotondo, Roma, Italy, and Dipartimento di Chimica, Università "La Sapienza" e sezione INFM, P.le A. Moro 5, 00185 Roma, Italy

The Journal of
Physical Chemistry C®

Reprinted from
Volume 111, Number 32, Pages 12045–12051

Enhancing the Gas-Sensing Properties of $(RuPc)_2$ Thin Films by Thermally Induced Morphological Stabilizing Effects

Amanda Generosi,*,† Barbara Paci,† Valerio Rossi Albertini,† Renato Generosi,† Paolo Perfetti,† Anna Maria Paoletti,‡ Gianna Pennesi,‡ Gentilina Rossi,‡ and Ruggero Caminiti§

Istituto di Struttura della Materia, CNR, Via del Fosso del Cavaliere 100, 00133 Roma, Italy, Istituto di Struttura della Materia, CNR, Via Salaria Km.29.5, Monterotondo, Roma, Italy, and Dipartimento di Chimica, Università "La Sapienza" e sezione INFM, P.le A. Moro 5, 00185 Roma, Italy

Received: May 7, 2007; In Final Form: June 15, 2007

We report on the use of thermal annealing to improve the behavior of NO_2 gas-sensing ruthenium phthalocyanine films at high temperatures. The approach used, based on the study of the effect of temperature on the film morphology, makes use of in situ energy dispersive X-ray reflectometry and atomic force microscopy. The results show that the morphological changes, induced by high working temperatures, strongly affect the material sensing ability. Furthermore, we demonstrate that the film morphology may be stabilized by thermal annealing treatments, thus enhancing the sensor performances in terms of response times and the capability to work at high temperatures.

Introduction

Much research is nowadays devoted to the development of devices able to discriminate NO_2 among other byproducts of the polluting emissions. In particular, phthalocyanines (Pc's), their metalloderivates (MPc's), and related compounds have shown the architectural flexibility and environmental stability suitable for technological applications.[1,2] The interest in developing gas detectors having Pc derivates as the chemically sensitive component of chemical/conductometric transduction systems is steadily increasing, since their electrical properties change upon exposure to oxidizing gases such as NO_2.[3−5] However, at present, several drawbacks have limited a massive development of Pc conductometric gas sensors. Indeed, their selectivity, sensitivity, response time, recovery rates, and behavior at room temperature still need to be improved.

In the present study, aiming to address some of the above crucial points, we focused on $(RuPc)_2$ phthalocyanine films.[6] Differently from the other insulating MPc's, the compound shows unconventional semiconducting properties ($\sigma_{RT} = 1 \times 10^{-4}\ \Omega^{-1}\ cm^{-1}$) and strong reactivity toward small molecules.[7] The $(RuPc)_2$ crystalline structure (as a powder and as a film)[7] and its behavior versus oxidizing gases such as NO_2 have been recently investigated with promising results, thus encouraging a deeper inspection of its properties as a sensor.[8−10]

Moreover, previous studies on various MPc's have shown that the gas-sensing characteristics of a specific compound are related to the morphology of the thin films, which is in turn affected by the preparation methods, the deposition conditions, and the postdeposition heat treatments.[11,12] In particular, heat annealing may cause structure reorganization or phase transformations, affecting the sensing properties of the films, and this effect is different depending on the system in study.[13,14]

* To whom correspondence should be addressed. E-mail: Amanda.Generosi@ism.cnr.it. Phone: +39 0649934146. Fax: +39 0649934153.
† CNR, Via del Fosso del Cavaliere 100.
‡ CNR, Via Salaria Km.29.5.
§ Università "La Sapienza" e sezione INFM.

In this work, joint in situ energy dispersive X-ray reflectometry (EDXR) and atomic force microscopy (AFM) studies on thin $(RuPc)_2$ films are presented. The two combined techniques enable observation of the real-time morphological changes of films during the postdeposition annealing procedure, in both the reciprocal and the direct space.

Experimental Section

EDXR. The EDXR technique is a powerful method to investigate monolithic and multilayered film structures.[15] Grazing incidence X-ray studies are highly sensitive to electron density gradients (irrespective of the crystalline or amorphous nature of the system investigated), allowing extraction of information on the system free surface and interface(s). In particular, they provide, with great accuracy, the mass density, the thickness, and the roughness of thin layers along the direction normal to the specimen surface.[16]

A simplified description of the basic principles of the physical phenomenon of total external reflection can be given in terms of classical optics, the exact description being given elsewhere.[15] Snell's law for refraction can be written as $n_1 \cos \alpha_i = n_2 \cos \alpha_r$ (α_i and n_1 being the incidence angle of the primary beam and the refractive index of the first medium and α_r and n_2 the reflection angle and the refractive index of the second medium). When a critical value of α_i is reached, called the critical angle α_c, then $\alpha_r = 0$, and if the first medium is air ($n_1 \cong 1$), then the Snell expression becomes $\cos \alpha_c = n_2$. In these conditions, the beam will not be refracted any longer but totally reflected. In the case of X-rays this optical model still applies, but a different definition of the refractive index is required: $n = 1 - \delta - i\beta = 1 - (\lambda^2/2\pi)\rho r_0 Z^2 - i(\lambda/4\pi)\mu$, where the real term δ is associated with the dispersion and the imaginary term β with the absorption of X-rays (negligible). Substituting the expression in the previous Snell law and taking into account that the incident angle is extremely small (so that the function $\cos \alpha$ can be expanded at the third order in McLaurin series), we obtain α_c/λ = constant. Under the same hypothesis of a small angle ($\sin \alpha \approx \alpha$), and since the scattering parameter is $q \cong$

10.1021/jp0734651 CCC: $37.00 © 2007 American Chemical Society
Published on Web 07/25/2007

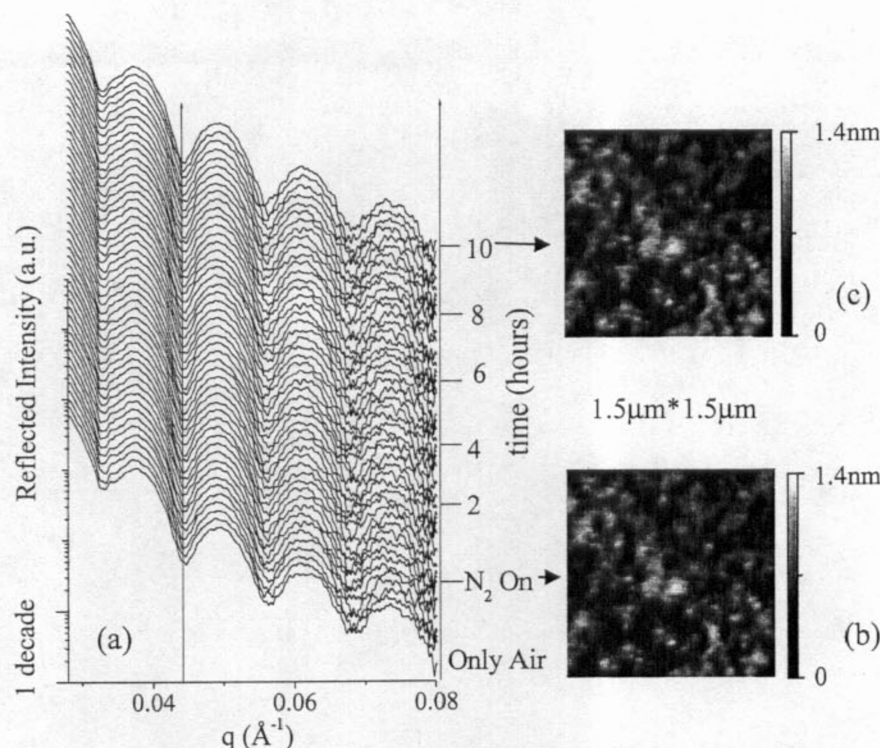

Figure 1. Right side: (a) Sequence of reflectivity patterns collected on a $(RuPc)_2$ thin film as a function of the scattering parameter q and of time, while N_2 molecules were fluxed (180 nmol/s) into the experimental chamber. As enhanced by the straight arrow, no modification of the EDXR spectra occurs. Left side: AFM images collected before the stability test (b) and after the sample was kept for 10 h in the N_2 atmosphere (c). No morphological modification is detected due to the N_2 gas flux or the X-ray exposure.

$4\pi(\sin\alpha)/\lambda$, X-ray total reflection occurs when the scattering parameter is below a critical value $q_c = 4\pi(\sin\vartheta)/\lambda$.

Therefore, at a very good approximation, in a total reflection experiment far from the absorption edge, the relevant parameter is not the critical angle alone, which changes with the X-ray energy, but rather the critical angle to wavelength ratio: $q = 4\pi(\sin\alpha)/\lambda = KE\sin\alpha$ (where E is the energy and the constant $K = 1.0136$ Å^{-1}/keV). Since a reflectivity measurement consists of collecting the reflected intensity as a function of the scattering parameter, two methods are available to perform the q scan and to draw the reflected intensity profile as a function of it: (i) using a monochromatic beam (fixed energy) and making an angular scan, called the angular dispersive (AD) mode; (ii) utilizing a continuum spectrum of radiation (often called a *white beam* in analogy with visible light), keeping the scattering angle fixed, referred to as the energy dispersive (ED) mode. Advantages and disadvantages of one method over the other have been fully discussed elsewhere,[17] but it is worth remarking that the experimental geometry remains unchanged during data collection, which is a fundamental advantage for in situ studies, as in this case.

The X-ray reflectometer is a noncommercial instrument[18] characterized by a very simple mechanical arrangement[19] consisting of two arms contained in the vertical plane, pivoting around a single central axis. The arms are moved by two linear actuators driven by step motors, and the tangent of the inclination angle is read by two linear encoders. Both the minimum step movement and the resolution of the encoders are 1 μm, leading to a minimum angle increment and reproducibility of $(4 \times 10^{-4})°$.[20] The "bremsstrahlung" of an ordinary X-ray tube (hot cathode W tube, Philips, model PW 2214/20)[21] is used as the radiation source, the working condition energy range being 25−55 keV. Despite the high energies available, the laboratory source produces limited X-ray fluxes (8 orders of magnitude less than in a third-generation synchrotron facility), thus ensuring that no radiation damage is induced on the MPc films.

The X-ray optical path is defined by four adjustable collimation slits (2 mm thick W slabs) mounted on the arms, limiting the angular divergence of the beam. The X-ray detection is accomplished by an EG&G solid-state detector whose sensitive part is a doped semiconducting high-purity germanium single crystal, acting as a photodiode. This kind of detector is able to encounter the number of photons reflected by the sample and, at the same time, to discriminate their energy, with a resolution of ca. 1.5% and a maximum counting rate of 10 kcounts/s.

The detector is connected via ADCAM hardware to a personal computer running a homemade software package[22] to visualize and record the data through a multichannel analyzer.

Film Deposition. Vacuum sublimation is generally used for depositing most (nonsubstituted) phthalocyanine compounds and is performed by heating a small quantity of purified material at temperatures ranging from 300 to 500 °C. All the $(RuPc)_2$ films examined in this paper were obtained by physical vapor deposition according to the standard procedure described elsewhere.[23] It basically consists of preparing the phthalocyanine films on Si[100] substrates by using an Edwards Auto 306 vacuum coater equipped with a diffusion pumping system. The growth was observed by an Edwards FTM5 film thickness monitor, measuring the change in the resonance frequency of a quartz crystal balance.

Results and Discussion

Postdeposition Annealing vs Sensing Efficiency. Recently intensive investigations have focused on the effect of high temperature (up to 225 °C) on the deposition and on the sensing characteristics of MPc films.[12,24] Indeed, the range of applicability of such materials as NO_2 detectors would be much enhanced

if higher sensing temperatures could be reached, nitrogen dioxide being a byproduct of combustion in vehicles and industrial plants. In particular, it has been demonstrated that annealing or heating treatments of the samples usually have a stabilizing effect on their electrical properties[25] and enhance their sensing abilities and recovery rates.[26] However, elevated temperatures may induce physical and chemical changes in the MPc films.[27] These effects are often modulated by the doping metal and, in turn, by the structural arrangement of the film.

To study the effect of postdeposition thermal treatments, the $(RuPc)_2$ thin films were annealed for 30 min in a N_2-enriched atmosphere at various temperatures, ranging from 130 to 240 °C (steps of 10 °C). Subsequently, joint gas-sensing experiments and EDXR measurements were performed to evaluate the consequences of heating on the gas−film interaction mechanism and on the sensing efficiency of the material toward NO_2 molecules. The NO_2 gas was diluted with high-purity N_2 down to a concentration of 50 ppm. The total gas flow rate was set to 220 nmol/s by a mass flow controller.

To control the sample stability in the experimental chamber and to verify that the $(RuPc)_2$ system is truly inert toward N_2 molecules, in situ reflectivity spectra were collected for several hours prior to the NO_2 insertion while N_2 molecules were fluxed (180 nmol/s), as visible in Figure 1. Moreover, an AFM study was performed on the as-deposited $(RuPc)_2$ film and after the stability test, the images being compared in the inset of Figure 1. As visible, no modification occurs, neither on the surface nor at a bulk level.

The morphological modifications occurring during the gas−film interaction and prior to this interaction, during the stability test, were obtained by an accurate Parratt[28] fit of the reflectivity spectra (collected for 500 s each) while the NO_2/N_2 gas mixture was flowed into the experimental chamber. In Figure 1, the real time evolution of the film thickness (dots) and roughness (triangles) is shown in the case of the $(RuPc)_2$ films thermally treated at 130, 170, and 180 °C, respectively. Some points, obtained by the fitting of the reflectivity patterns collected during the stability test, are shown to validate the use of N_2 molecules as a driving inert gas. For all temperatures ranging between 130 and 170 °C, the film morphology exhibited the same behavior (see Figure 2a,b): a "breathing-like" expansion of the film bulk. Indeed, the progressive thickening of the films interacting with NO_2 molecules is well fitted by a sigmoidal Boltzmann curve (line). This behavior describes a single-step mechanism consistent with a bulk diffusion process. Previous studies[29] have evidenced that, at the first cycle, "as-deposited" $(RuPc)_2$ films show a two-step morphological response to the exposure to NO_2 gas, i.e., superficial adsorption and bulk diffusion. The former is an irreversible process and is not present during the second cycle of interaction with the NO_2 molecules, i.e., after a thermal reset of the film following the first activating cycle. Therefore, an a priori thermal treatment acts, from the point of view of the irreversible film surface modifications, as a thermal reset procedure.

Moreover, in the present case, in analogy to the case of a second cycle, the time evolution of the film roughness behavior is consistent with an initial thickening of the film due to the bulk diffusion of NO_2 molecules, which slightly disorder the free surface. When the maximum diffusion speed is reached, the surface roughness saturates.

The first effects of the postdeposition thermal annealing at low temperatures ($T < 180$ °C) are thus evident: the efficiency of the sensing material is enhanced, since its response time is reduced and undesired surface gas−film interactions are prevented.

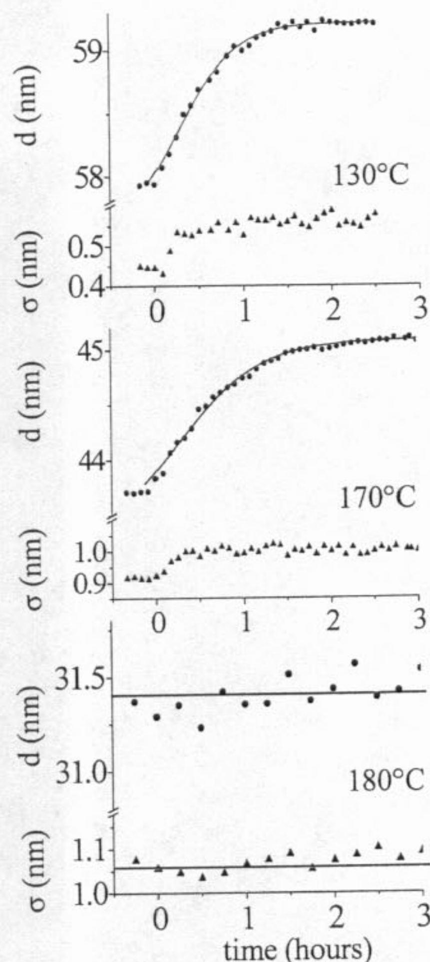

Figure 2. Time evolution of the morphological parameters d (circles) and σ (triangles) deduced by the Parratt fitting of reflectivity spectrum sequences, collected on differently thermally treated $(RuPc)_2$ films during exposure to a 50 ppm NO_2 gas flux. The continuous lines represent the fitting of the thickness evolution.

However, this morphological monitoring of the film treated at 180 °C clearly evidences, in this case, that no gas−film interaction occurs at all, so that the $(RuPc)_2$ is no longer able to detect the pollutant molecules. Indeed, the film thickness and roughness do not exhibit any variation during the exposure to the NO_2 gas flux, their values being unchanged (Figure 2c, red line) within the experimental error. The explanation for this experimental result may be that the thermal treatment in these conditions is too aggressive and the thin film structure, playing a fundamental role in the detection process, may have been corrupted.

Role of Morphology. To verify the above hypothesis, an in situ EDXR study was performed during the annealing process (in a N_2 atmosphere at 180 °C) to observe the effect of heating at this temperature on the $(RuPc)_2$ film morphology. An expressly designed oven, provided with X-ray-transparent windows, was used to accomplish the annealing under a controlled atmosphere and, at the same time, to collect the reflectivity spectra. Furthermore, AFM images were collected before the annealing process and during the thermal treatment to observe the morphological behavior also from a microstructural point of view. A noncommercial air operating atomic force microscope was used.[30]

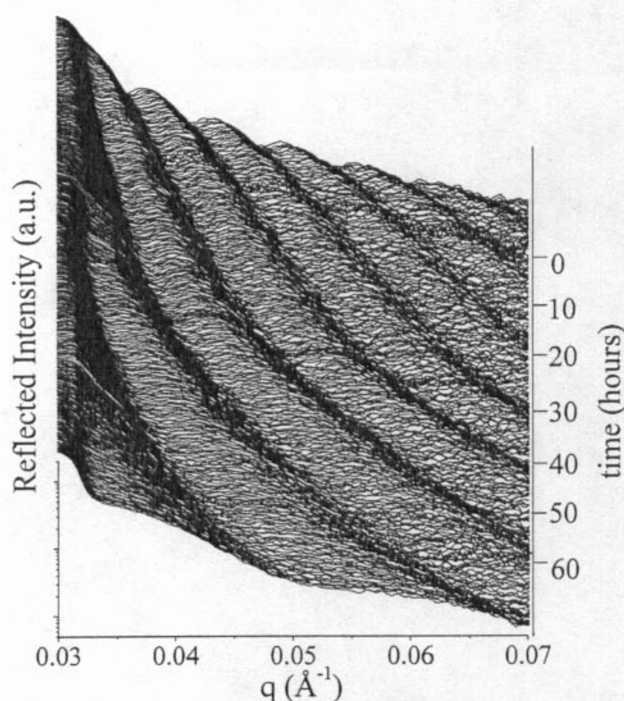

Figure 3. Sequence of reflectivity patterns collected as a function of the scattering parameter q and of time, during an isothermal treatment at 180 °C. As visible by the arrow connecting the minima of the first oscillation, as time passes by the oscillation shifts toward lower q values, i.e., the film gets thinner.

The 180 °C annealing process lasted 72 h, and the sampling by EDXR was performed every 15 min. In Figure 3, the 3D sequence of reflectivity spectra collected during the thermal treatment is plotted as a function of the scattering parameter and of time. As visible by the naked eye, as time passes by, the Kiessig fringes[31] slowly move toward higher q values (their wavelength increases). A rough estimation of the film thickness can be obtained by the approximated relation $d \cong 2\pi/\Delta q$. Therefore, we can state that the $(RuPc)_2$ film gets thinner during the annealing process. This can be easily explained in terms of the thermal energy applied to the film, which is sufficient to sublimate the surface $(RuPc)_2$ molecules, and then removed by the N_2 stream. By the Parratt fit of each reflectivity spectrum, the time evolution of thickness and roughness is obtained (parts a and b, respectively, of Figure 4). The film continues to get thinner and thinner until a critical thickness (20 nm) is reached. At this point, the adhesion forces binding the $(RuPc)_2$ molecules to the Si substrate are strong enough to contrast the volatilization effect, so that no more molecules are released from the surface. Meanwhile, the surface roughness apparently decreases during the annealing process, but it gets back to its original value as soon as the sublimation is concluded. Indeed, since the EDXR technique is sensitive to the electron density in the scattering volume, the $(RuPc)_2$ sublimated molecules in contact with the surface contribute to the reflected signal as well as the ones in the solid state. Therefore, during the sublimation process the film solid surface appears smoother due to the fact that $(RuPc)_2$ molecules in the solid state and free molecules coexist. This apparently reduces the surface roughness.

In Figure 4, the change of the film thickness and roughness during the first 30 min of annealing is evidenced. As shown, the morphological changes are quite remarkable, being characterized by a linear decrease of both the thickness and the roughness.

Moreover, the AFM images collected on the sample as-deposited and after 30 min, 8 h, and 24 h of thermal treatment

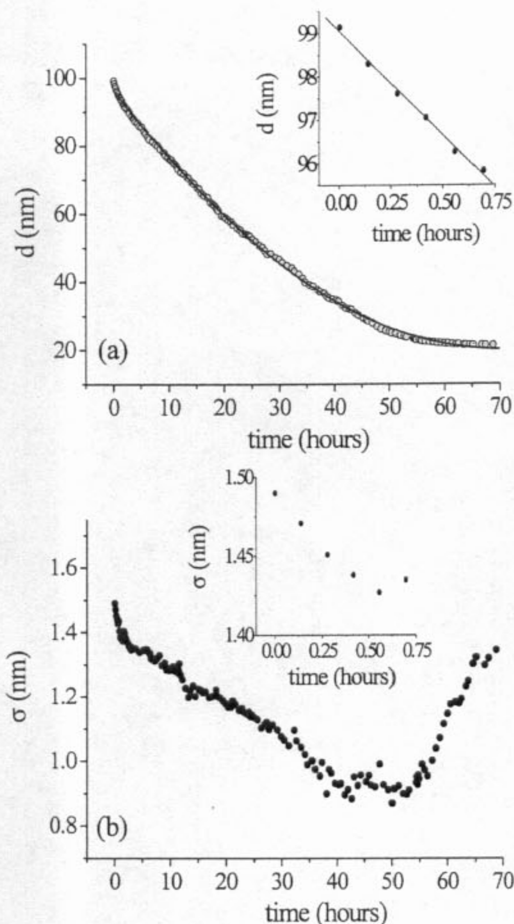

Figure 4. Time evolution of the morphological parameters thickness (a) and roughness (b) of a $(RuPc)_2$ film during the 180 °C thermal treatment, as deduced by the reflectivity data processing. In the insets the morphological behaviors observed during the first 30 min of thermal treatment are evidenced.

at the same temperature (parts a, b, c, and d, respectively, of Figure 5) clearly support these considerations. The homogeneous texture of the as-deposited sample, being characterized by regular grains of average dimensions 100 nm lateral × 0.7 nm vertical, after 30 min of thermal treatment turns into a system of larger aggregates, produced by the coalescence of the initial small grains (average size 220 nm lateral × 10 nm vertical).

When the annealing is performed for more than 30 min, the surface is still characterized by the molten texture analyzed in Figure 5b, but randomly large aggregates are formed. As visible in Figure 5c, when 8 h has passed, disordered clusters (average dimensions being 220 nm lateral × 20 nm vertical) appear to be randomly distributed on the surface. Finally, when the $(RuPc)_2$ film has been heated for 24 h, such aggregates have increased in size (characteristic dimensions being 250 nm lateral × 20 nm vertical) and cover the surface homogeneously.

This evidence supports the previous hypothesis that a thermal treatment at 180 °C for 30 min corrupts the $(RuPc)_2$ film morphology, thus inhibiting the sensing capabilities, which are strongly related to the quality of the surface morphology. Indeed, the AFM technique has been applied to different Pc systems in the past few years to investigate the role of surface morphology on the gas-sensing characteristics of the films.[32] The analysis of the surface roughness (rms) as well as the average and maximum grain height and dimension provided information on the number of adsorption sites and on the conductive path, the modification of these parameters strongly affecting their sensing abilities.[33]

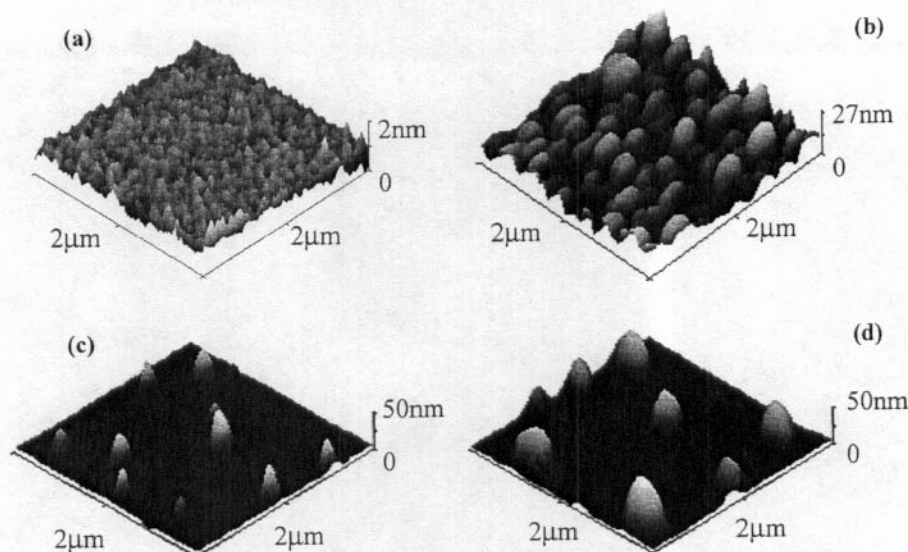

Figure 5. AFM images collected on an as-deposited $(RuPc)_2$ film (a) and after 30 min (b), 8 h (c), and 24 h (d) of 180 °C thermal treatment.

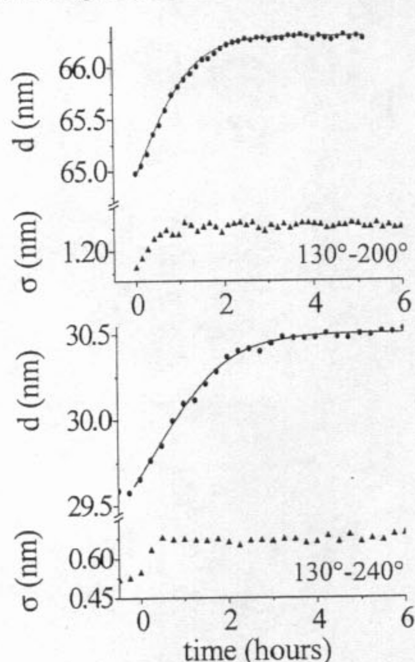

Figure 6. Time evolution of the morphological parameters d (circles) and σ (triangles) deduced by the Parratt fitting of reflectivity spectra sequences, collected on 130 °C thermally pretreated $(RuPc)_2$ films submitted to an annealing process. The upper image is relative to a film annealed at 240 °C and the lower one to a film treated at 200 °C.

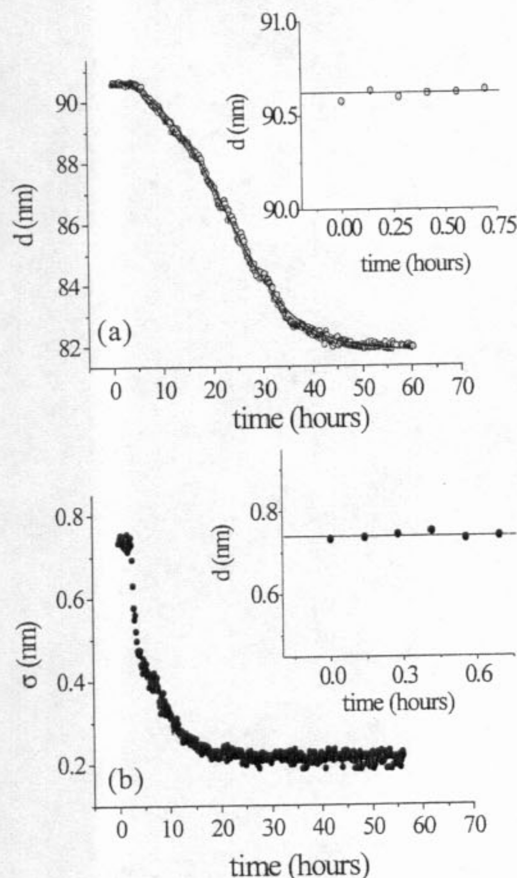

Figure 7. Time evolution of the morphological parameters thickness (a) and roughness (b) of a $(RuPc)_2$ 130 °C pretreated film during the 180 °C thermal annealing. The parameters are deduced by the Parratt fit of the reflectivity spectra collected during the thermal treatment. In the insets the morphological behaviors observed during the first 30 min are evidenced, no modification being visible.

Stabilizing Effect of the 130 °C Thermal Pretreatment. Thermal treatments have been widely documented in the literature to stabilize the different MPc crystalline phases,[34,35] either α or β, and to make them more resistant to further heating.[5,13-16] Starting from these considerations, a thermal stabilizing procedure was applied to $(RuPc)_2$ to stabilize the morphology, which has proved to be a critical parameter, and enhance the performance of the material as a sensing device.[25]

A series of thin $(RuPc)_2$ films were deposited on Si and underwent two subsequent heating processes: at first, all samples were submitted to a 130 °C thermal pretreatment for 30 min in a N_2 atmosphere and, then, were left in air until they had cooled to room temperature. As a second step, the films were heated once more at temperatures ranging from 180 to 260 °C for 30 min. After the second heating, the samples were measured by EDXR while being exposed to a NO_2/N_2 gas molecule mixture (50 ppm).

From the analysis of the evolution of the morphological parameters of these samples, it appears that, due to the pretreatment at 130 °C, the $(RuPc)_2$ films retain their sensing ability despite being heated to 240 °C. Indeed, as visible in parts a and b of Figure 6, after the second treatment at 200 and 240 °C, the breathing-like expansion of the lattice already

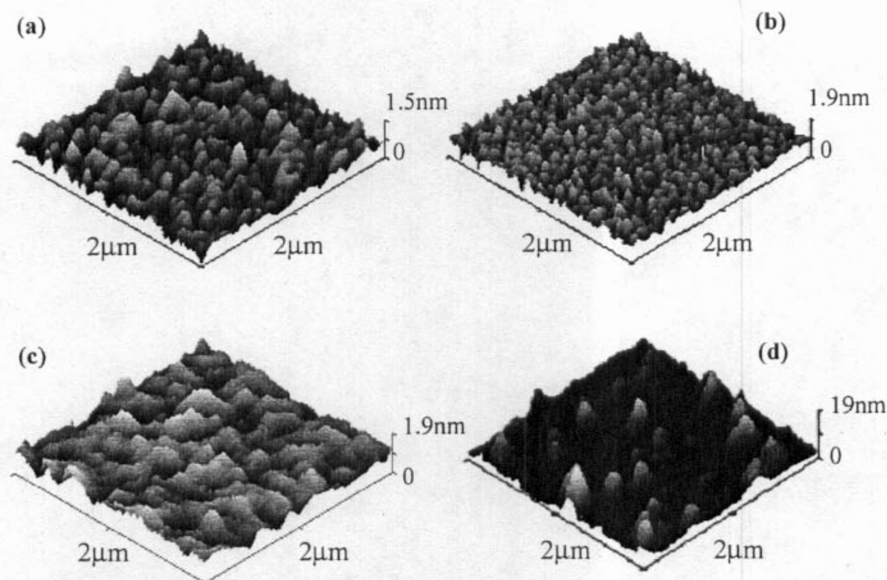

Figure 8. AFM images collected on a 130 °C thermally pretreated $(RuPc)_2$ film (a) and after 30 min (b), 8 h (c) and 24 h (d) of 180 °C thermal treatment.

observed is reproduced. Furthermore, the efficiency is preserved, and also the surface roughness exhibits the same profile shown in part a or b of Figure 2. This behavior is completely different from that of nonpretreated samples, that is, samples submitted directly to a single thermal treatment at 180 °C. In the latter case, indeed, the sample had been corrupted by heating at a lower temperature (180 °C vs 200 or even 240 °C) with consequent loss of its sensing capability.

To verify whether the 130 °C thermal treatment is actually responsible for the retention of the sensing ability as a consequence of the stabilizing effect induced on the $(RuPc)_2$ film morphology, another sample was stabilized at that temperature. Subsequently, this $(RuPc)_2$ film underwent the annealing treatment at 180 °C as previously described, during the collection of the EDXR spectra. The sequence of reflectivity patterns was collected over 3 days (72 h) with a time resolution of 15 min.

By the Parratt fit of each EDXR spectrum, the time evolution of the thickness and roughness were deduced and are reported in parts a and b, respectively, of Figure 7. Both parameters evolve in a different manner if compared to the parameters plotted in Figure 4, the most peculiar feature being the presence of a long induction time (7 h) before the first $(RuPc)_2$ molecules leave the film surface. Furthermore, once the process is activated, it evolves on the same time scale as before, but this film loses only 12% of its initial thickness, while the previous sample, without the 130 °C pretreatment, lost 80% of its initial thickness. This indicates the cohesion within the $(RuPc)_2$ molecules, inside the film, is strongly increased, and consequently, the morphology becomes less sensitive to heating. The initial stages of the morphologic parameter evolution are highlighted in the insets of Figure 7, where d and σ vs t are shown during the first 30 min of the thermal treatment. As visible, no modification occurs and the values are constant in this time interval. Furthermore, the AFM images, collected on the as-deposited film, after the 130 °C stabilizing heating, after 8 and 24 h at 180 °C, confirms these considerations. As visible in Figure 8a (the as-deposited film image), the texture show a very regular granular structure (100 nm lateral × 0.7 nm vertical size), the small particles being well separated from each other with an average corrugation perfectly coherent with the EDXR roughness estimation. After 30 min of thermal pretreatment at 130 °C, no surface deterioration is detectable. An example of the images is shown in Figure 8b. The surface texture is more defined after this pretreatment, and the granular structures are more resolved, still homogeneously covering the surface, with an average size of 60 nm lateral × 0.7 nm vertical.

After the pretreatment at 130 °C, the sample was submitted to an annealing at 180 °C. Consistently with the EDXR results, the morphology appears unchanged during the first 7 h at 180 °C. Moreover, after 8 h (Figure 8c), the granular microstructures begin to coalesce into larger clusters, their average size being 120 nm lateral × 1.2 nm vertical. The texture is very regular all over the surface, and the corrugation value decreases as previously deduced by the EDXR measurements.

After 24 h at 180 °C, the surface is visibly deteriorated, see Figure 8d, and the formation of inhomogeneous aggregates, whose characteristic average dimensions are 120 nm lateral × 10 nm vertical, is observed.

This is more evidence of the fundamental role that the morphology plays in the sensing process.

Conclusions

The results of combined EDXR−AFM studies on the structural stability of $(RuPc)_2$ film gas sensors upon thermal treatments are reported.

The study evidences that it is not the temperature that directly discriminates whether the material retains its sensing ability, but the morphology changes induced by heating. When the morphology is corrupted, the $(RuPc)_2$ films are not able to act as sensing devices any longer. However, it is possible to stabilize the morphology, thus enhancing the performances of the $(RuPc)_2$ films, by thermally pretreating the films at 130 °C for 30 min. In this way, the first induction cycle disappears, the response times are shorter, and the material is stable to further annealing up to 240 °C.

In conclusion, the results reported demonstrate how annealing treatments may enhance the performances of such sensor materials, reducing their response time and allowing high-temperature working conditions, as required to monitor NO_2 emissions from combustion in vehicles and industrial installations.

References and Notes

(1) Guillard, G.; Simon, J.; Germain, J. P. *Coord. Chem. Rev.* **1998**, *178−180*, 1433.

(2) Ferraro, J. R.; Williams, J. M. *Introduction to Synthetic Electrical Conductors*; Academic Press: Orlando, FL, 1987; p 219.

(3) Capobianchi, A.; Paoletti, A. M.; Pennesi, G.; Rossi, G. *Sens. Actuators, B* **1998**, *48*, 333.

(4) Leznoff, C. C. In *Phthalocyanines Properties and Applications*; Lever, A. B. P., Eds.; VCH: New York, 1996; Vols. 1−4.

(5) Sompson, T. R. E.; Russel, D. A.; Cook, M. J.; Horn, A. B.; Thorpe, S. C. *Sens. Actuators, B* **1995**, *29*, 353.

(6) Rawling, T.; McDonagh, A. *Coord. Chem. Rev.* **2007**, *251*, 1129.

(7) Capobianchi, A.; Paoletti, A. M.; Pennesi, G.; Rossi, G.; Caminti, R.; Ercolani, C. *Inorg. Chem.* **1994**, *33*, 4635.

(8) Rossi Albertini, V.; Generosi, A.; Paci, B.; Perfetti, P.; Rossi, G.; Capobianchi, A.; Paoletti, A. M.; Caminiti, R. *Appl. Phys. Lett.* **2003**, *82* (22), 3868.

(9) Generosi, A.; Paci, B.; Rossi, V.; Perfetti, P.; Paoletti, A. M.; Pennesi, G.; Rossi, G.; Caminiti, R. *J. Appl. Phys.* **2006**, *99*, 1.

(10) Generosi, A.; Paci, B.; Rossi Albertini, V.; Perfetti, P.; Pennesi, G.; Paoletti, A. M.; Rossi, G.; Capobianchi, A.; Caminiti, R. *Appl. Phys. Lett.* **2005**, *86*, 114106.

(11) Lee, Y.-L.; Tsai, W.-C.; Chang, C.-H.; Yang, Y.-M. *Appl. Surf. Sci.* **2001**, *172*, 191.

(12) Lee, Y.-L.; Hsiao, C.-Y.; Chang, C.-H.; Yang, Y.-M. *Sens. Actuators, B* **2003**, *94*, 169.

(13) Liu C. J., Hsieh J. C., Ju Y. H. *J. Vac. Sci. Technol., A* **1996**, *14*, 753.

(14) Ottaviano, L.; Lozzi, L.; Phani, A. R.; Ciattoni, A.; Cantucci, S.; Di Nardo, S. *Appl. Surf. Sci.* **1998**, *136*, 81.

(15) Rossi Albertini, V.; Paci, B.; Generosi, A. *J. Phys. D: Appl. Phys.* **2006**, *39*, R461.

(16) Tolan, M. *X-Ray Scattering from Soft-Matter Thin Films*; Springer Tracts in Modern Physics, Vol. 148; Springer: Heidelberg, Germany, 1999.

(17) Caminti, R.; Rossi Albertini, V. *Int. Rev. Phys. Chem.* **1999**, *18* (2), 26.

(18) Felici, R.; Cilloco, F.; Caminiti, R.; Sadun, C.; Rossi Albertini, V. Italian Patent No. RM 93 A000410, 1993.

(19) Caminiti, R.; Sadun, C.; Rossi Albertini, V.; Cilloco, F.; Felici, R. *Proceedings of the 25th National Congress of Physical Chemistry*, University of Cagliari: Cagliari, Italy, June 17−21, 1991; p 221.

(20) Felici, R. *Rigaku J.* **1995**, *12* (1), 11.

(21) Nishikawa, K.; Iijima, T. *Bull. Chem. Soc. Jpn.* **1984**, *57*, 1750.

(22) Bailo, D. Internal Report; ISM, CNR: Rome, 2006.

(23) Caminiti, R.; Capobianchi, A.; Marovino, P.; Paoletti, A. M.; Pennesi, G.; Rossi, G. *Thin Solid Films* **2001**, *382*, 74.

(24) Lee, Y.-L.; Hsiao, C.-Y., Chanh, C.-H.; Yang, Y.-M *Sens. Actuators, B* **2003**, *94*, 169.

(25) El-Nahass, M. M.; El-Deeb, A. F.; Abd-El-Salam, F. *Org. Electon.* **2006**, *7*, 261.

(26) Lee, Y.-L.; Sheu, C.-Y.; Hsia, R.-H. *Sens. Actuators, B* **2004**, *99*, 281.

(27) Tongpool, R. *Thin Solid Films* **2003**, *438−439*,14.

(28) Parratt, L. G. *Phys. Rev.* **1954**, *95*, 359.

(29) Generosi, A.; Paci, B.; Rossi Albertini, V.; Perfetti, P.; Paoletti, A. M.; Pennesi, G.; Rossi, G.; Caminiti, R. *Appl. Phys. Lett.* **2006**, *88*, 104106.

(30) Cricenti, A.; Generosi, R. *Rev. Sci. Instrum.* **1995**, *66*, 2843.

(31) Kiessig, H. *Ann. Phys.* **1931**, *10*, 769.

(32) Liu, C. J.; Shih, J. J.; Ju, Y. H. *Sens. Actuators, B* **2004**, *99*, 344.

(33) Grzadziel, L.; Zak, J.; Szuber, J. *Thin Solid Films* **2003**, *436*, 70.

(34) Peumans, P.; Uchida, S.; Forrest, S. R. *Nature* **2003**, *425*, 158.

(35) Yang, F.; Shtein, M.; Forrest, S. R. *Nat. Mater.* **2005**, *4*, 37.